



ARL-TR-8226 • Nov 2017



Fabrication and Characterization of the US Army Research Laboratory Surface Enhanced Raman Scattering (SERS) Substrates

**by Mikella E Farrell, Karen Grutter, Michael A Powers, and
Paul M Pellegrino**

Approved for public release; distribution is unlimited.

NOTICES

Disclaimers

The findings in this report are not to be construed as an official Department of the Army position unless so designated by other authorized documents.

Citation of manufacturer's or trade names does not constitute an official endorsement or approval of the use thereof.

Destroy this report when it is no longer needed. Do not return it to the originator.



Fabrication and Characterization of the US Army Research Laboratory Surface Enhanced Raman Scattering (SERS) Substrates

by Mikella E Farrell, Michael A Powers, and Paul M Pellegrino
Sensors and Electron Devices Directorate, ARL

Karen Grutter
Laboratory for Physical Sciences, College Park, MD

REPORT DOCUMENTATION PAGE

*Form Approved
OMB No. 0704-0188*

Public reporting burden for this collection of information is estimated to average 1 hour per response, including the time for reviewing instructions, searching existing data sources, gathering and maintaining the data needed, and completing and reviewing the collection information. Send comments regarding this burden estimate or any other aspect of this collection of information, including suggestions for reducing the burden, to Department of Defense, Washington Headquarters Services, Directorate for Information Operations and Reports (0704-0188), 1215 Jefferson Davis Highway, Suite 1204, Arlington, VA 22202-4302. Respondents should be aware that notwithstanding any other provision of law, no person shall be subject to any penalty for failing to comply with a collection of information if it does not display a currently valid OMB control number.

PLEASE DO NOT RETURN YOUR FORM TO THE ABOVE ADDRESS.

1. REPORT DATE (DD-MM-YYYY) November 2017		2. REPORT TYPE Technical Report		3. DATES COVERED (From - To) 1 January 2016–31 May 2017	
4. TITLE AND SUBTITLE Fabrication and Characterization of the US Army Research Laboratory Surface Enhanced Raman Scattering (SERS) Substrates				5a. CONTRACT NUMBER	
				5b. GRANT NUMBER	
				5c. PROGRAM ELEMENT NUMBER	
6. AUTHOR(S) Mikella E Farrell, Karen Grutter, Michael A Powers, and Paul M Pellegrino				5d. PROJECT NUMBER	
				5e. TASK NUMBER	
				5f. WORK UNIT NUMBER	
7. PERFORMING ORGANIZATION NAME(S) AND ADDRESS(ES) US Army Research Laboratory ATTN: RDRL-SEE-E 2800 Powder Mill Road Adelphi, MD 20783-1138				8. PERFORMING ORGANIZATION REPORT NUMBER ARL-TR-8226	
9. SPONSORING/MONITORING AGENCY NAME(S) AND ADDRESS(ES)				10. SPONSOR/MONITOR'S ACRONYM(S)	
				11. SPONSOR/MONITOR'S REPORT NUMBER(S)	
12. DISTRIBUTION/AVAILABILITY STATEMENT Approved for public release; distribution is unlimited.					
13. SUPPLEMENTARY NOTES					
14. ABSTRACT Capabilities for timely and accurate sensing and identifying of unknown materials at point of contact and in real time are critically important for the US Department of Defense and other first responders and thereby aid in the determination of proper reaction. Technologies that include Raman-based sensing offer one potential means to work toward accomplishing this goal. Of the several commercially available Raman-based sensors, none have yet to be a successfully demonstrated universal sensor for US Army-relevant sensing. In this report we discuss the fabrication process of the US Army Research Laboratory's (ARL's) Surface Enhanced Raman Scattering (SERS) substrates for potential sensing and identification of unknown materials. We demonstrate that the substrate was SERS-active and able to detect a standard SERS analyte. We also demonstrate that the ARL SERS substrate is comparable to the previously commercially available Klarite substrate. A discussion of future works highlights the potential use of this substrate for Army-relevant detection and identification of unknown materials.					
15. SUBJECT TERMS Surface Enhanced Raman Scattering, SERS, Raman, Klarite, sensing					
16. SECURITY CLASSIFICATION OF:			17. LIMITATION OF ABSTRACT UU	18. NUMBER OF PAGES 52	19a. NAME OF RESPONSIBLE PERSON Mikella E Farrell
a. REPORT Unclassified	b. ABSTRACT Unclassified	c. THIS PAGE Unclassified			19b. TELEPHONE NUMBER (Include area code) 301-394-0948

Standard Form 298 (Rev. 8/98)
Prescribed by ANSI Std. Z39.18

Contents

List of Figures	v
Acknowledgments	vi
1. Introduction	1
1.1 Raman and SERS Background	1
1.1.1 Types of SERS Surfaces	2
1.1.2 Nanoparticles and Self-Assembly	3
1.1.3 Designed Nanostructures	4
1.1.4 Photonic SERS Substrates	5
1.1.5 Hybrid SERS Surfaces/Polymer-Based Coatings/Bio-Inspired Materials	5
1.2 US Army-Relevant Applications of SERS-Hazard Detection	7
1.3 Assessing SERS Substrate: ARL/Edgewood Chemical Biological Center (ECBC)–Developed Methodology	9
1.4 SERS Substrates	10
2. Experiment	11
2.1 Chemicals	11
2.2 Mask Design	11
2.3 Substrates Fabrication	11
2.4 Raman Measurement System	12
2.5 Data Analysis	12
3. Results and Discussion	12
3.1 Klarite Substrate Characterization	12
3.2 Mask Design	13
3.3 ARL SERS Substrate Fabrication	14
3.4 ARL SERS Substrate Characterization	17
4. Conclusions	20

5. References	21
Appendix. Supplemental Information	35
List of Symbols, Abbreviations, and Acronyms	43
Distribution List	44

List of Figures

Fig. 1	Examples of SERS use in a) biological sensing using FONs, b) hazard/explosive detection with common explosives TNT, PETN (pentaerythritol tetranitrate), and RDX as measured on a Klarite substrate, c) chemical sensing with known SERS standards trans-1,2-bis(4-pyridyl)-ethylene (BPE) and benzoic acid (BA) as measured on a Klarite substrate, d) examples of biological sensing on several variations of commercially available Klarite substrates (encompassing standard and next-generation Klarite substrates), e) chemical imaging using a SERS-based nanoimaging probe from work at the University of Maryland Baltimore County, and f) examples of just a few types of SERS substrates that can be used for SERS sensing and have been tested at ARL for Army-based sensing needs.....	8
Fig. 2	Klarite substrate: a) SEM image demonstrating single inverted pyramid, b) AFM data demonstrating topography of substrate surface, and c) AFM data with tilted view of substrate surface	13
Fig. 3	a) Schematic for mask used to fabricate ARL SERS wafer and b) an example of diced wafer substrate size with active area (pink) and nonactive area (white).....	13
Fig. 4	Example microscope images collected from a “dummy” substrate following lithography shown at a) high and b) low magnification.....	15
Fig. 5	SEM images of the KOH etched ARL SERS substrate wafer. The different quadrants are seen in a–c. In d) a higher-magnification image demonstrates etching at the bottom of the inverted pyramid feature..	16
Fig. 6	SEM images of metalized ARL SERS substrate at various magnifications.....	17
Fig. 7	ARL SERS substrate transmission data.....	18
Fig. 8	a) Example SERS spectrum BPE, b) SERS of BPE on various quadrants of ARL SERS substrate, c) SNR for each quadrant at various bands, and d) data presented in graph format	19

Acknowledgments

Thanks to all co-authors for helpful discussions and clean-room training.

1. Introduction

Surface Enhanced Raman Scattering (SERS) can offer sample detection and identification solutions to applications that include medical diagnostics, military situations in which there are possible chemical, biological, and explosive materials on site, and even environmental contamination concerns. For SERS to function as an accurate, reliable, and reproducible technology for all of these research areas, it is important to have access to a dynamic (i.e., able to be tailored to current and emerging materials) and universal (i.e., able to be applied to a large range of unknowns) SERS substrates. To this end, considerable investment has been put into developing SERS substrates that are easily and inexpensively manufactured, demonstrate signal reproducibility from substrate to substrate and lot to lot, and are capable of being used in a host of environments with diverse target materials and still demonstrate consistently good SERS signal enhancement. In this report we briefly discuss some current methodologies for fabricating SERS-based substrates, discuss efforts at the US Army Research Laboratory (ARL) to fabricate a SERS-based substrate, and characterize the performance of the ARL SERS substrate via plasmon absorbance data and by measuring the SERS signal from a common analyte material.

1.1 Raman and SERS Background

Raman-based sensing offers many advantages for Army-relevant sensing applications. Raman is a spectroscopic technique that relies on inelastic scattering from a laser light source. It is a technique commonly used to provide a unique fingerprint spectrum from which sample material identity can be determined. Other advantages of Raman over some other spectroscopic techniques include little to no sample preparation being necessary, the ability to collect signal from relatively small sample volumes, no sample degradation, the ability to be used with several laser sources, and that it does not suffer from interferences from water.¹⁻⁵ Despite these advantages, for many of the Army-relevant materials to sense, Raman is a relatively weak phenomenon; therefore, signal-enhancing techniques like SERS can be used instead.⁶⁻¹²

The SERS effect was observed and documented in the 1970s, and a full understanding of the effect was later described. An enhancement of the Raman signal occurs when a target or molecule of interest is brought into close or direct contact with a surface that has a layer of roughened (i.e., nanostructured, particle-size distribution) metals on the nanoscale surface. When the surface is interrogated, the interaction of the molecule and surface can lead to primarily chemical and electromagnetic (EM) enhancements. The EM effect occurs with a collective

oscillation of conduction electrons, also known as surface plasmon resonance (SPR). The EM effect is the dominant contributor to the overall signal enhancement. The chemical enhancement occurs when there is a charge transfer resonance between the molecule and the metalized surface. These effects can also be coupled. The SPR can be modified by varying parameters like the size, shape, and metal of the SERS substrate.

SERS is an analytical technique that is well-suited to the molecular identification of a variety of compounds by revealing specific vibrations within the molecule to produce a fingerprint spectrum from which sample component identification is possible. This vibration-based technique is applicable in a variety of environments, as it does not suffer from interferences from water and is relatively insensitive to the excitation wavelength employed (i.e., no reliance on visible absorption). Under ideal conditions, SERS signal enhancement has been reported to be up to 14 orders of magnitude greater than spontaneous (i.e., nonenhanced) Raman, allowing for single molecule detection. This signal enhancement from SERS is achieved by depositing an analyte onto (or in close proximity to) a nanoscale roughened metal surface, irradiating the surface, and then taking advantage of both chemical and EM enhancements that occur. SERS spectra can be used to not only detect analytes of interest, but also to understand a bit about the environment in which they are found.

1.1.1 Types of SERS Surfaces

SERS substrates can be fabricated from a host of different techniques.^{2,7,11-16} Early techniques used included the deposition of electro-chemically roughened metal electrodes and various colloid prepared processes (usually silver [Ag] or gold [Au] materials). These fabrication techniques resulted in surfaces consisting of randomized “hot spots” or areas of increased overall SERS signal enhancements. Because of the random nature of some of these early, more simplistic SERS substrates, there was significant variation in substrate performance and reproducibility. However, with current technological advances there has been a push for the design and fabrication of more “designed” SERS substrate surfaces that exhibit uniform structure and SERS signal enhancement. Examples of designed SERS surfaces include those that are fabricated using bottom-up chemical synthesis and top-down nanofabrication techniques. Also, there is an increasing research trend in the design of hybrid SERS surfaces that incorporates them into plasmonic nanostructures and can even incorporate bio-inspired materials for increased selectivity.

1.1.2 Nanoparticles and Self-Assembly

Metal nanoparticles are a readily available means for fabricating SERS substrates. Metal nanoparticles are particularly advantageous to use because they frequently demonstrate good SERS signal enhancement, substrate signal stability, and can be easily and cheaply fabricated. Typically, Au or Ag are the metals of choice for SERS signal enhancement using visible laser sources because their plasmon resonances lie in the visible region.

The process of fabricating Au or Ag nanoparticles is frequently considered a “bottom-up” synthesis technique. Nanoparticles can be synthesized following a simple process involving coprecipitation of a soluble metal salt and then adding a reducing agent. Common examples of these types of reactions include Lee and Meisel synthesis as well as the Fren and Natan techniques.¹⁷⁻²⁵ Additionally, by changing parameters of the synthesis process it is possible to tailor the nanoparticle shape, size, and overall structure. These nanoparticles can also be tailored to be composed of different metals, thus providing increased SERS signal, varied functionality, and even different separation methods (e.g., when incorporating magnetic materials). This has interesting implications for selecting and tailoring properties of the nanoparticles to that of the system in which the SERS signal will be measured (i.e., laser wavelength employed, specific application, and measurement environment). Challenges for these types of nanoparticles can include degradation over time due to the rapid oxidation of Ag nanoparticles, variance in reproducibility (i.e., spot to spot, substrate to substrate, and batch to batch), and issues with particle aggregation and overall SERS signal.

Another example of a SERS nanoparticle consists of a metallic core surrounded by some functional shell, thus forming a shell nanoparticle structure. Advantages of these types of nanoparticles are that the outer shell of the nanoparticle can protect the metal core from environmental impacts, additional functionalization/tagging options on the shell exist, and in some cases the shells might help with decreasing aggregation, if desired.

As mentioned, it is possible to control the experimental conditions in the nanoparticle synthesis process to change such parameters as nanoparticle size and overall shape. Implementing these controls in the fabrication process allows for the design and growth of shapes including nanorods, nanowires, nanocubes,^{26,27} nanoprisms,²⁸ and nanostars.²⁹⁻³¹ These sorts of shapes offer some advantages like tailored plasmon bands, the ability to couple several individual nanomaterials to create substrates that exhibit increased SERS signal enhancement factors, and the option to preferentially pack particles onto substrate surfaces with some known density/orientation and thus possibly control the number of “hot spots” that an

analyte can access. Because of the host of advantages, various SERS nanoparticle shapes are being used in research areas that include imaging,^{32–35} biosensors,^{10,36–44} drug delivery,^{45–54} and various photothermal therapies.^{45,50–52,55–59}

1.1.3 Designed Nanostructures

Significant research efforts have also been concentrated on better directing the optimization of the substrate surface from which the SERS enhancement occurs. Based in part on experimental and theoretical efforts, the directed fabrication of SERS platforms has focused on modifying the feature size,^{60–62} spacing between objects, geometry and shape of structures, identity and incorporation of metals on the surface,⁶³ feature height, and the characteristics of the foundation layer on which the architecture is fabricated. Variation in some of these parameters has been shown in some cases to result in very large changes to the overall SERS signal-enhancing capabilities of the substrate surface. Efforts continue to focus on developing an understanding of how these parameters can combine to result in a highly reproducible and sensitive SERS substrate. As research continues to push and improve the overall sensing capabilities of the SERS surface, corresponding research continues to push toward development of a uniform, reproducible (SERS signal response, substrate architecture), and mass-produced platform necessary to facilitate widespread incorporation of SERS in viable dynamic (current and emerging targets) and universal (applicable to a range of target types) sensing platforms.

Some of the challenges associated with the fabrication of SERS substrates from chemical synthesis include sensitivity (detection limits, response to a range of target types), tenability (ability to be used with a range of laser sources, target sizes), stability (overall SERS signal enhancement over time), possible background interference from synthesis materials, and reproducibility. However, with advances in nanoscale fabrication technology, some of these challenges can be partially overcome by implementing design controls (architecture of substrate, substrate material, how materials are loaded). Examples of these fabrication platforms include lithographically produced structures, such as nanospheres, nano-antennas, and nanogap arrays, and designed structures such as film over nanoparticles (FONs).^{64–68} Nanosphere lithography can be carried out several ways. Van Duyne and coworkers have shown a substrate structure in which nanotriangle structures are created by depositing a monolayer of nanospheres, a metal layer, and then removing the nanosphere mask.^{69,70} FONs have also been fabricated by depositing a monolayer of nanoparticles onto a surface and then depositing/adhering a layer of metal onto this surface. The spacing of this monolayer surface can also be controlled by imparting functionality to the nanoparticle, thus ensuring some

specific predetermined interparticle spacing. Some interesting work has also been demonstrated with multilayer FONs made up of varying metal layers and spacers. These multilayer FONs demonstrate increased lifetime and overall SERS enhancement factors as compared with a single layer of individual metal.^{68,71-76}

Specifically designed SERS surfaces can also be fabricated from optical nano-antenna surfaces. Optical nano-antennas are typically devices that are able to convert free-propagating optical radiation into localized energy at the hot spot, which is basically a resonant plasmonic structure. This increase in the EM field can lead to an increase in vibrational signal from the molecules that are located at or in close proximity to the hot spot. There are several examples in the literature^{49,50,63,77-89} of these types of SERS surfaces, and they can range in shape from “bow-tie”-like structures to plasmonic nano-antennas.

Another example of a specifically designed surface includes the nanogap array. Traditionally, nanogap arrays^{90,91} are fabricated by electron beam lithography (EBL). Following etching, the platform can be chemically etched and desired metals deposited. Using EBL, it can be very challenging to fabricate reproducible and repeatable gaps of the correct/designed dimensions. To overcome this, some researchers have been able to combine EBL with electrochemical methods to better control the gap spacing.^{92,93} By running current through an EBL-fabricated gap array, it has been shown to be possible to impact atomic positions within a lattice. Other groups have also had success controlling the spacing of nanogaps by employing femtosecond lasers and nano-imprinting techniques.⁹⁴⁻⁹⁸ Advantages of using these techniques include increased reproducible enhancement factors because of the significant control of the surface and the potential to create reproducible SERS substrates over a larger surface area.

1.1.4 Photonic SERS Substrates

With technological advances in the areas of integrated photonics, researchers are increasingly looking for means to fabricate Raman, Raman-based, and SERS surfaces onto devices like dielectric gratings and photonic crystals. Advantages of these types of devices include increased SERS enhancement factors, the ability to create a dense array of hotspots, and smaller sensor area. Integrated photonic SERS substrates might become a reality as technological advances and foundry fabrication methods become more widely available and accepted.

1.1.5 Hybrid SERS Surfaces/Polymer-Based Coatings/Bio-Inspired Materials

One of the main challenges in the design and fabrication of a sensor platform is analyte selectivity and sensitivity. To answer this challenge, researchers have

looked into imparting selectivity and sensitivity into SERS substrates using polymer-based coatings and biological recognition elements.

Polymer-based SERS sensing has been demonstrated to be effective at sensing Army-relevant materials.^{14,22,58,85,99} Polymer SERS sensing can be achieved by coating a SERS-active surface with a polymer that only allows access by selected materials or the preferential trapping of selected, predetermined materials to the SERS sensing surface (molecular imprinting polymer/SERS work),⁵ incorporating coatings onto metal nanoparticles, and SERS hydrogels materials.

A high degree of sensor selectivity can be achieved by using biological recognition elements (i.e., biomimetic sensing). Such sensing entails the adaptation of biological principles, designs, selective sensitive materials, and signal processing schemes merged with artificial (nonbiological material) sensors. Biomaterials can be used in SERS substrates as a functionalized material to aid in sensing and as the platform in which the SERS sensing is possible. Advantages of these materials include the potential for label-free detection and identification, elimination of significant sample preparation/specific reagents, and no interference from water.

Biomimetic sensing recognition elements can include more-traditional antibody sensing motifs and, increasingly, peptides as the biological recognition element. These SERS biosensors^{80,100–102} based on hybrid nanostructures have been used in research to study proteins,^{103–105} cancer markers,^{33,106} trace explosives,¹⁰⁷ various genes, chemical warfare species, bacteria,^{60,108–114} diagnostic markers, environmental pollutants, glucose monitoring,^{102,115} and stress-related biomarkers in Soldiers.¹⁰²

Antibodies^{82,89,116} have been traditionally used in these SERS-based sensor platforms, as they are typically more familiar to many researchers. Challenges with antibody-based SERS sensors can include robustness of the recognition element and dynamic adaptability of the element to a variety of threat materials. Increasingly, researchers are using peptides as SERS recognition elements.^{64,89,117–119} Peptides are short (<50) chains of amino acids. Generally, in sensing platforms, peptides are advantageous to use because they 1) are stable and robust in environments where other functionalization chemistries are labile, 2) can be easily synthesized, 3) are cost- and time-efficient, 4) can be easily modified to recognize a target, 5) are well characterized, and 6) have been shown to easily immobilize to various surface platform materials (e.g., metals, plastics, fabrics, and tissue samples).

Other examples of bio-inspired SERS substrates include utilizing photosynthetic marine micro-organisms such as diatoms in periodic structures,^{120–124} anemone type structures,¹²⁵ coated plant extracts⁸³ functioning as probes, incorporated into flower

petals¹²⁶ and leaves, and nanoparticle coated onto seed,^{127,128} and even onto metal-coated insect wings.^{86,87}

1.2 US Army-Relevant Applications of SERS-Hazard Detection

To effectively support and carry out the mission, Soldiers and support staff must have safe food, air, water, and a secure environment. To ensure this safety it is important to not only detect, but also to identify threat material so that proper countermeasures can be taken. One way that this can be accomplished is through employing sensitive and specific sensing techniques such as SERS. SERS applications to Army-relevant sensing include measuring analyte materials like biological targets, energetics, and chemical hazards such as toxic industrial chemicals and materials. A universal (i.e., applicable to and useful in the full range of possible threats and conditions) sensor solution is desired because it simplifies the logistical and training burdens, which are preeminent Army concerns. Such an ideal SERS sensor does not yet exist, but we believe that through continued research work, technological advances, and collaborations with partners throughout the Department of Defense, academia, and industry we can produce a much more “ideal” sensor for future Army-sensing needs.

Figure 1 depicts several examples of Army-relevant sensing completed at ARL. ARL has been in a unique position to investigate SERS substrates fabricated from a host of different fabrication techniques ranging from FONs, fiber-optic bundle, materials grown through various deposition techniques, sputtered surfaces, ink-jet printing, as well as a few examples of commercially available substrates.

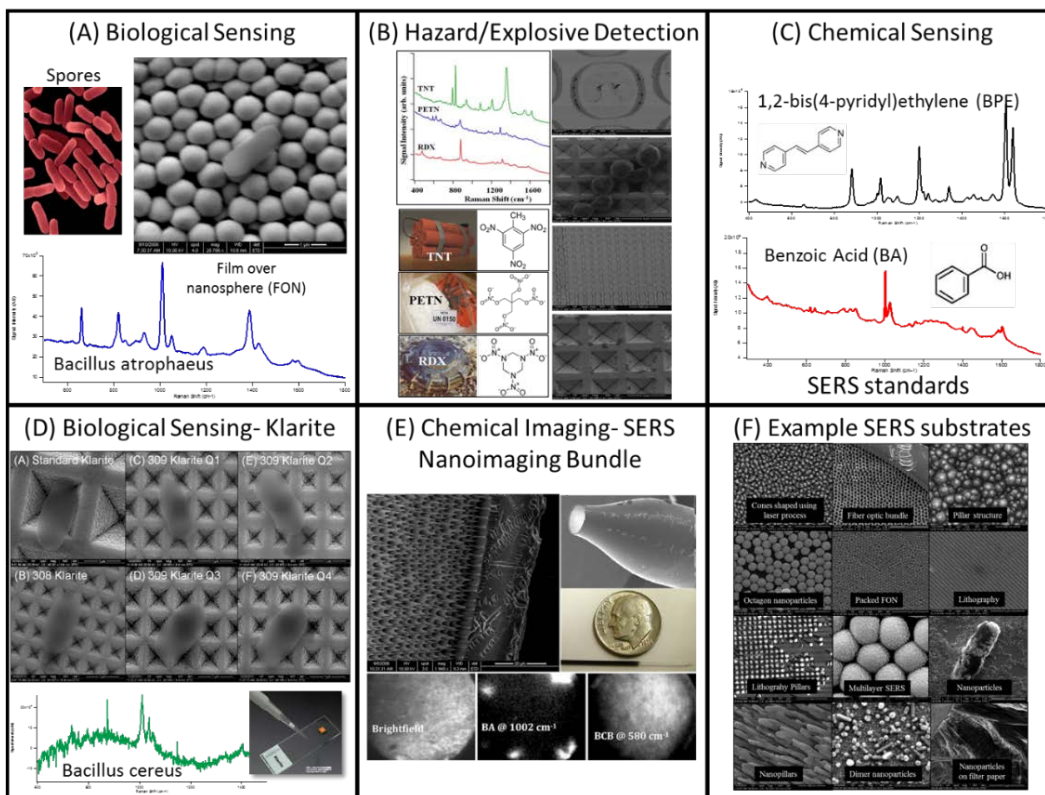


Fig. 1 Examples of SERS use in a) biological sensing using FONs, b) hazard/explosive detection with common explosives TNT, PETN (pentaerythritol tetranitrate), and RDX as measured on a Klarite substrate, c) chemical sensing with known SERS standards trans-1,2-bis(4-pyridyl)-ethylene (BPE) and benzoic acid (BA) as measured on a Klarite substrate, d) examples of biological sensing on several variations of commercially available Klarite substrates (encompassing standard and next-generation Klarite substrates), e) chemical imaging using a SERS-based nanoimaging probe from work at the University of Maryland Baltimore County, and f) examples of just a few types of SERS substrates that can be used for SERS sensing and have been tested at ARL for Army-based sensing needs

One recent successful example demonstrating the use of SERS substrates for Army-relevant sensing used modified bifunctional peptides to capture hazardous materials (explosives, biomaterial) for measurements on a functionalized Au surface.^{1,2,71,129,130} In these experiments, bifunctional peptides, designed to anchor onto an Au surface with an extending “capture” peptide sequence for capturing hazardous materials like TNT or protective antigen, were bound onto a SERS substrate surface. A solution containing the hazardous material was exposed to the surface, the surface was washed, and the resulting SERS spectrum from the bound target material was measured. With this proof-of-principle demonstration, the utility of such a sensing platform for sensing Army-relevant hazardous materials was demonstrated.

1.3 Assessing SERS Substrate: ARL/Edgewood Chemical Biological Center (ECBC)–Developed Methodology

The “ideal” SERS substrate has yet to be commercially available; however, there are several examples of SERS substrates that are or have been available (from commercial, academic, or government sources), and many of these substrates demonstrate both advantages and disadvantages. At ARL we have had the opportunity to evaluate several of these substrates for Army-relevant use. These substrates were tested using a methodology developed in collaboration with government researchers at ECBC in conjunction with a Defense Advanced Research Projects Agency–funded SERS fundamentals program.¹³¹ This technique is not the only means by which a SERS substrate can be assessed and the evaluation criteria are not universally relevant, but it did offer performers a starting point from which additional assessments could be performed.

Following the steps laid out in this developed methodology, SERS substrates were exposed to several predetermined SERS active materials, and the resulting spectra were collected and used to fabricate a concentration curve.¹³¹ Briefly, ECBC and ARL collaborators published *Surface-Enhanced Raman Scattering (SERS) Evaluation Protocol for Nanometallic Surfaces* to provide the SERS sensing community both analytical and spectroscopic figures of merit to compare the sensitivity and reproducibility of various SERS substrates.¹³¹ The evaluation metric selected was the ratio of the area of a peak (1200 cm^{-1}) in the spectrum of BPE to the ethanol in which the BPE was dissolved. This protocol provides a means to determine, for a particular type of SERS substrate and on a given instrument (Renishaw microscope) using standardized acquisition conditions (10-min soak time), the minimum detectable concentration of an analyte and to determine SERS reproducibility, from spot to spot on a given substrate (5 measurements collected per substrate), from substrate to substrate, and over time.

These data were used to provide a qualitative means of comparing different substrate types. This value was meant to be used in addition to other evaluation criteria to determine how well the SERS substrates performed. Other considerations included 1) determining if the targets could get into close contact with the substrate surface (e.g., were biological spore samples able to access “hot spots” across the SERS substrate surface), 2) measuring if there was significant background from the substrate itself (fabrication contamination), determining if the substrate surface was single use or could be regenerated (how easily could metals be removed and reapplied), 3) testing for surface delamination when exposed to solution (many Army targets can be in solution; i.e., biomaterials), 4) measuring overall SERS active surface area (how large of an area did the sample need to be in contact with), and

5) getting an estimate on typical substrate lifetime (how long could it be used after sitting out in a lab bench environment). Also, for these measurements it is understood that a SERS measurement detects a 2-D area while a comparable bulk measurement detects molecules in a 3-D volume. Because of nonuniformity (i.e., structure, number of hotspots, surface area) of the evaluated SERS surfaces, it was difficult to calculate the number of adsorbed molecules on the SERS surface and in the detected volume of a normal Raman measurement; therefore, the assessment was an empirical protocol meant to just give a starting point number for evaluation. The authors understood that this assessment was not necessarily the best protocol to follow for the evaluation of all SERS substrates. For this evaluation, the SERS enhancement value was defined as the ratio of the concentrations that produced, on a particular instrument, the same instrument responses for normal Raman scattering as SERS scattering. The military is interested in detecting warfare agents and identifying false positives and false negatives; therefore, receiver operating characteristic curves for analysis were also determined.

Frequently, many of these SERS substrates demonstrated good overall SERS signal enhancement; however, researchers had no path toward rapidly scaling up the substrate production rate. Lacking alternatives, for most Army applications and material assessments, commercially available SERS substrates—such as, the Klarite substrate (previously available from Renishaw)—were often used.

1.4 SERS Substrates

Some successfully fabricated and uniformly reproducible SERS substrates have been demonstrated with previously commercially available Klarite substrates (Renishaw).^{132–136} These substrates were developed using silicon semiconductor fabrication techniques.¹³⁶ Klarite substrates are fabricated using a well-defined technique in which a silicon dioxide mask is defined by optical lithography, and then the wafer is selectively and anisotropically etched using potassium hydroxide (KOH). The process results in an array of highly reproducible inverted pyramid structures.¹³⁶ These array pyramids are reported to have “hot spots” or “trapped plasmons” located inside the wells.¹³⁶ These substrates have been previously characterized at ARL using atomic force microscopy (AFM) analysis and plasmon data collection. From our previous work,² AFM images have been used to characterize inverted pyramids approximately 1.47 μm wide and 1 μm wide. Plasmon absorbance bands are located at 577 and 749 nm, thus demonstrating the usefulness of this substrate with a range of realistic excitation sources. Additionally, because of the fabrication process used, under ideal conditions these substrates have demonstrated typical relative standard deviations (RSDs) ranging from 10% to 15%.¹³⁶ While these substrates demonstrate a high degree of substrate

reproducibility and very low substrate background (SERS signal and surface morphology), realistic application requires greater sensitivity. The calculated enhancement factor for common SERS standard targets on the Klarite substrate is around 10^6 . Another challenge is that these substrates are no longer commercially available; therefore, researchers must work with materials previously purchased.

To increase the overall sensitivity of these substrates and demonstrate the ability to regenerate SERS surfaces, recent ARL work completed in collaboration with researchers at the University of Maryland Baltimore County on regenerating the metal surface is discussed in this report. The response of the original SERS substrates is compared with those of a regenerated surface. Original substrate data were collected when the substrates were first procured and regeneration data were collected on older but unused substrates.

2. Experiment

2.1 Chemicals

Chemicals used included BPE, ethanol, and water. All chemicals were used as received without further purification. Chemicals used in SERS substrate fabrication were supplied from ARL clean-room stock.

2.2 Mask Design

An ARL mask was designed at ARL and fabricated by Compugraphics with the following dimensions:

- Quadrant I: hole = $1.5\ \mu\text{m}$, space = $0.5\ \mu\text{m}$, period = $2\ \mu\text{m}$ (original Klarite dimensions)
- Quadrant II: hole = $1.3\ \mu\text{m}$, space = $0.7\ \mu\text{m}$, period = $2\ \mu\text{m}$
- Quadrant III: hole = $1.5\ \mu\text{m}$, space = $1.5\ \mu\text{m}$, period = $3\ \mu\text{m}$
- Quadrant IV: hole = $2\ \mu\text{m}$, space = $2\ \mu\text{m}$, period = $4\ \mu\text{m}$

2.3 Substrates Fabrication

To fabricate the ARL SERS substrates, several instruments available in the ARL clean room were employed, including the following: Plasma Therm 790+ oxide/nitride plasma-enhanced chemical vapor deposition (PECVD; silicon nitride [SiN] deposition); Nanometrics NanoSpec 3000 PHV; EVG 120 Resist Processing Cluster; EVG 120 Resist Processing Center; Brewer Science hot plate; Karl Suss

MA6/BA6 contact aligner; hot plate; Karl Suss–Flood exposure; TAM H Developer (Hood 11) exposure development; MetroLine M4L; Unaxis ULR 700 Etch PM 3 (nitride etch); isopropyl alcohol (IPA)/acetone clean; Piranha Photoresist Strip; KOH etch; hydrochloric acid clean; hydrofluoric acid (HF) etch (49% premade solution); CHA Evaporator, and scanning electron microscopy (SEM).

2.4 Raman Measurement System

At ARL the SERS and Raman spectra were collected using a Renishaw Raman microscope. The Renishaw microscope has 3 lasers operating at 514, 632, and 785 nm, respectively. Spectra were collected using the NIR 785-nm laser unless otherwise indicated. The laser light was focused onto the sample using a 20× objective, exposures were 30 s in length, and one accumulation was collected per spot. Samples were moved into position using a motorized XYZ translational stage. Spectra were collected and the instrument was run using Wire 2.0 software operating on a dedicated computer.

2.5 Data Analysis

Data analysis was achieved using IgorPro 6.0 software (Wavemetrics).

3. Results and Discussion

3.1 Klarite Substrate Characterization

Researchers at ARL were interested in mimicking the pattern of the Klarite substrate, as well as exploring the SERS response from substrates with a slightly different design. SERS substrates from Klarite were selected as the baseline because researchers at ARL had extensive history working with and characterizing this platform, and they have proven active from several previous studies. The Klarite substrate consists of a series of inverted pyramids, the tips of which are where “hot spots” are located (Fig. 2 is an example SEM of a Klarite substrate). The inverted pyramids are approximately 1.47 μm wide and 1 μm deep. Plasmon absorbance bands are located at 577 and 749 nm, thus demonstrating the usefulness of this substrate with a range of excitation sources. These substrates have demonstrated typical RSDs ranging from 10% to 15% based on work previously done at ARL. While these substrates demonstrate a high degree of substrate reproducibility and very low substrate background (SERS signal and surface morphology), practical analyte sensitivity is lacking. The calculated enhancement factors for common SERS standard targets on the Klarite substrate is around 10^6 .

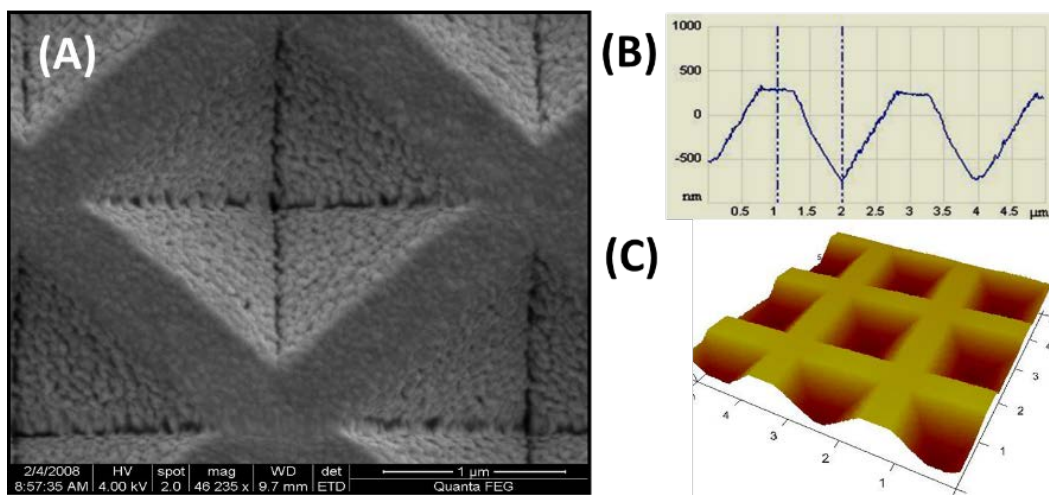


Fig. 2 Klarite substrate: a) SEM image demonstrating single inverted pyramid, b) AFM data demonstrating topography of substrate surface, and c) AFM data with tilted view of substrate surface

3.2 Mask Design

The ARL SERS substrate was designed at ARL, and a mask (Compugraphics) was fabricated with variable dimensions (Fig. 3). This mask design was meant to give researchers a “baseline” to compare the ARL SERS substrate to the previously commercially available Klarite, as well as explore some of the fabrication capabilities in the ARL clean room. To fabricate the ARL SERS substrate, a plain Si wafer with $\langle 100 \rangle$ orientation was used.

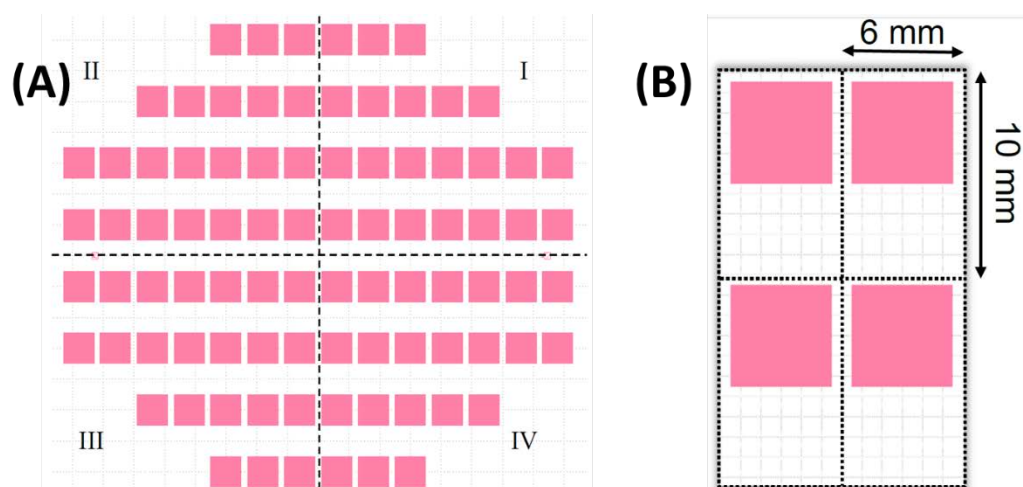


Fig. 3 a) Schematic for mask used to fabricate ARL SERS wafer and b) an example of diced wafer substrate size with active area (pink) and nonactive area (white)

3.3 ARL SERS Substrate Fabrication

To fabricate the ARL SERS substrate, it was necessary to first deposit nitride onto the wafer (see the Appendix for complete information). This was accomplished using the Plasma Therm 790+ oxide/nitride PECVD (nitride deposition). It was determined that nitride be deposited at a rate of 12.01 nm/min; therefore, the wafer needed about 10 min for a final thickness of approximately 100 nm. After deposition, thickness was verified using the Nanometrics NanoSpec 3000 PHV. The wafer was cleaned with acetone, IPA, and water to prepare it for the next processing step. Next, the resist needed to be deposited onto the wafer surface. This was accomplished using the EVG 120 Resist Processing Cluster with parameters for a 4-inch wafer, HMDS (hexamethyldisilazane) bake, and AZ5214E resist spun at 4000 rpm with an “area” dispense, 110 °C soft bake for 1 min. The resist used for this was the AZ 5214E Photoresist, which is intended for liftoff techniques that call for a negative side-wall profile. The reversal bake moderately cross-links the exposed resist, making the developed structures thermally stable up to approximately 130 °C. Due to the comparably low-resist film thickness, the process parameter window for an undercut is rather small, thus requiring some optimizations in the exposure dose and the reversal bake parameters. This resist is also a good option if the resolution required is in the sub- μm size range (adapted from <http://dvh.physics.illinois.edu/pdf/AZ5214E.pdf>).¹³⁷ After the resist has been deposited, it is necessary to bake it to prevent mask sticking; this is done using the Brewer Scientific hot plate, baking at 110 °C for 1 min.

Using the Karl Suss MA6/BA6 contact aligner, the designed mask features can be put onto the resist-covered wafer. For this step it was determined that the lamp produces about 8.9 MW/cm. Therefore, for effective contact alignment it was necessary to expose the mask for 7 s. Then the wafer was placed on the hot plate for 2 min at 120 °C to complete an image reversal bake. Next the silicon wafer was subjected to a flood exposure to expose the resist to a blanket of radiation for 30 s. Then the resist was developed by using the tetra methyl ammonium hydroxide (TMAH)/AZ 300MIF developer, which is a metal-ion-free industry-standard 0.261-N TMAH-based developer that is surfactant free. The wafer was placed in AZ 300MIF developer for 30 s, placed in water, and then dried. Using a yellow filter on a microscope, the resulting pattern was characterized. Next the photoresist-covered wafer was cleaned and any residues removed using the MetroLine M4L/IPC plasma photoresist stripper using recipe “5214.descum.2min”. The effectiveness of this cleaning step was evaluated via microscope inspection of the surface (Fig. 4 is an example of a cleaned substrate surface).

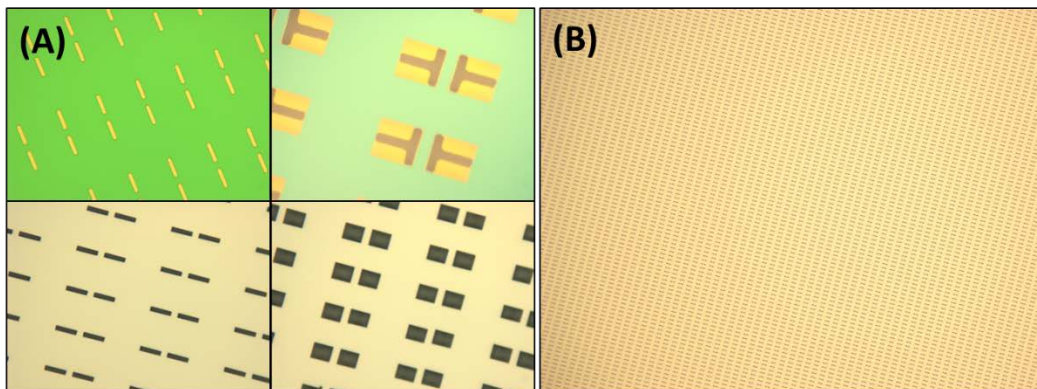


Fig. 4 Example microscope images collected from a “dummy” substrate following lithography shown at a) high and b) low magnification

Next the SiN layer needed to be etched, accomplished using the Unaxis VLR 700 Etch PM3-Dielectric etch. For this step it is important to first run the process on a dummy wafer to condition the instrument. After conditioning, half of the process (20 s) was run on the actual wafer and then stopped to determine the etch rate. The Nanospec was used to confirm the etch rate of approximately 3.25 nm/s. Then the etching process was completed for an additional 28 s. The wafer was then cleaned using an IPA/acetone clean. The wafer was placed in a large dish of acetone twice (5 min each time), followed by soaking in IPA for 5 min. Next, Piranha acid processing was completed to remove any photoresist and any organic contaminants that might be on the wafer. During this process small bubbles developed across the wafer surface after it was submerged into the acid wash. This process took approximately 20 min.

In the next step the features on the ARL SERS substrate were etched via a standard KOH bath. The 45% KOH solution was premade, and the process was done at 80 °C. The wafer was briefly wetted in water and then processed in KOH for 15 min. Then it was washed in water and immersed in an HCl (hydrogen chloride):water solution to remove any additional precipitate that formed. After etching, the wafer features were inspected under a microscope to ensure that the bottom well of features had been completely etched. Example SEM images from the various quadrants are shown in Fig. 5a–c. In Fig. 5c, the etching process is demonstrated with the bottom of the pyramid feature appearing to come to a point (not flat). Next the Nanospec was used to determine the final thickness of the SiN.

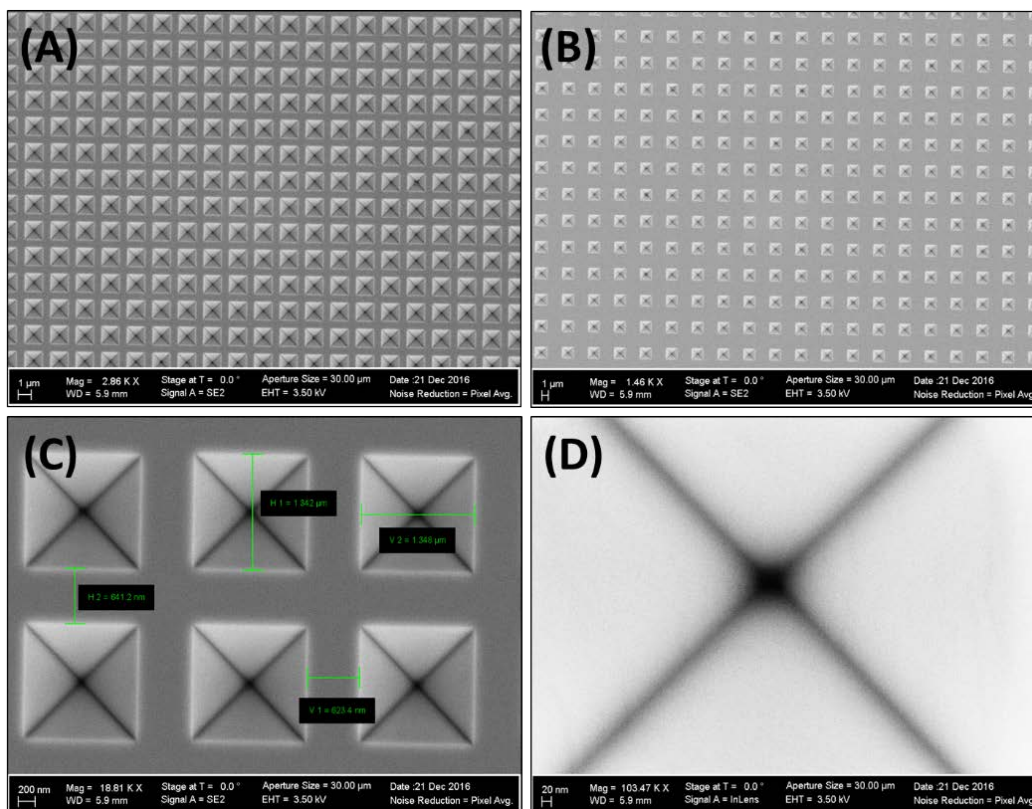


Fig. 5 SEM images of the KOH etched ARL SERS substrate wafer. The different quadrants are seen in a–c. In d) a higher-magnification image demonstrates etching at the bottom of the inverted pyramid feature.

Next the SiN mask layer was removed using a 49% premade HF wash, immersing the wafer for approximately 3 min. During this processing step, a color change from yellow to silver across the wafer was observed as the etching occurred, leaving the wafer surface highly hydrophobic.

After cleaning, the wafer was ready for metal processing using the CHA e-Beam Vacuum Evaporator system. In this process, chromium (Cr) and Au are deposited sequentially onto the wafer surface. For this process, approximately 20 nm of Cr and 500 nm of Au was deposited onto the wafer surface. Following metal deposition the metalized wafer surface was characterized via SEM imaging. Figure 6 shows the roughened substructure across the ARL SERS wafer. It might be possible to additionally optimize the roughness of this surface to increase overall SERS signal enhancement by changing parameters such as amount of deposited metal and the evaporation/sputter rate of metals deposited.

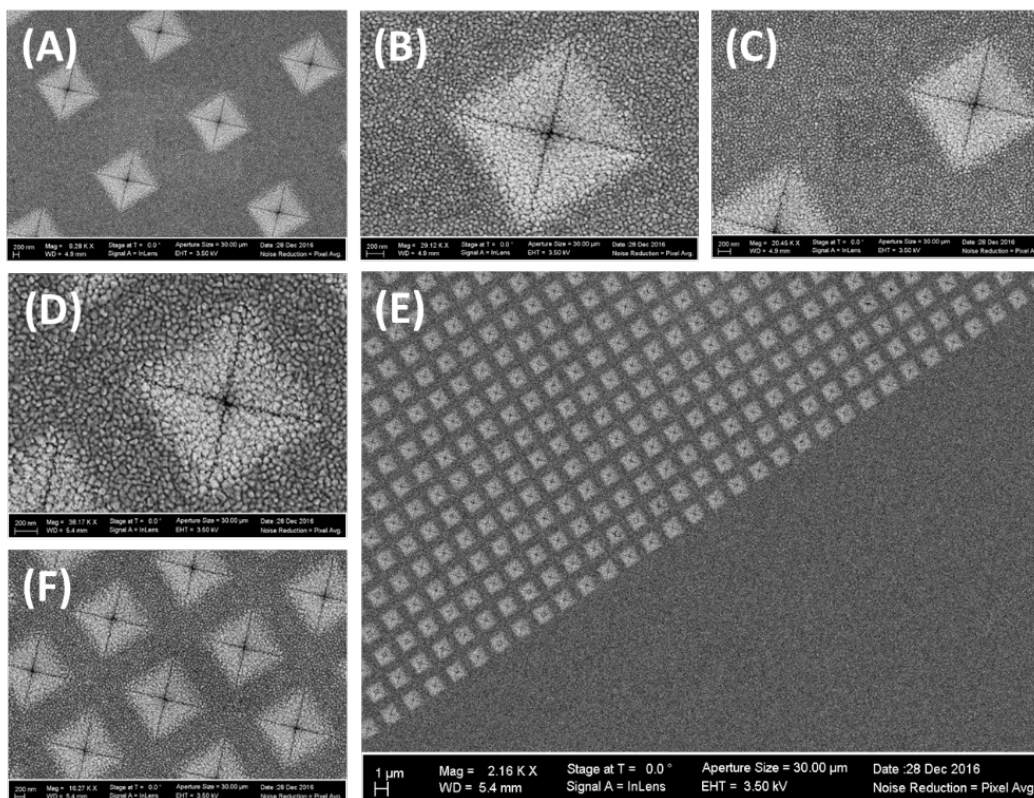


Fig. 6 SEM images of metalized ARL SERS substrate at various magnifications

3.4 ARL SERS Substrate Characterization

Following fabrication, it was necessary to characterize the performance of the ARL SERS substrate. This was accomplished by collecting absorbance data and SERS signal data (Fig. 7). Based on these data, Quadrant 1 has main absorbance bands occurring at 558 and 774 nm, Quadrant 2 has main bands occurring at 509 and 715 nm, Quadrant 3 has main bands occurring at 563 and 812 nm, and Quadrant 4 has main bands occurring at 542 and 728 nm. The dimensions of Quadrant 1 are meant to mimic those of the original Klarite SERS substrate. A standard Klarite substrate has main absorbance bands that occur at 577 and 749 nm, which is very comparable to those measured on ARL SERS substrate Quadrant 1. With the range of absorbance bands measured and the laser wavelengths available at ARL with the benchtop Renishaw microscope, it can be concluded that for the 785-nm laser, Quadrants 1 and 3 should result in greater overall SERS signal enhancement measurements. Quadrant 2 should perform best with a 514-nm laser. It is clear that the 633-nm laser would be best used with Quadrants 2 and 4.

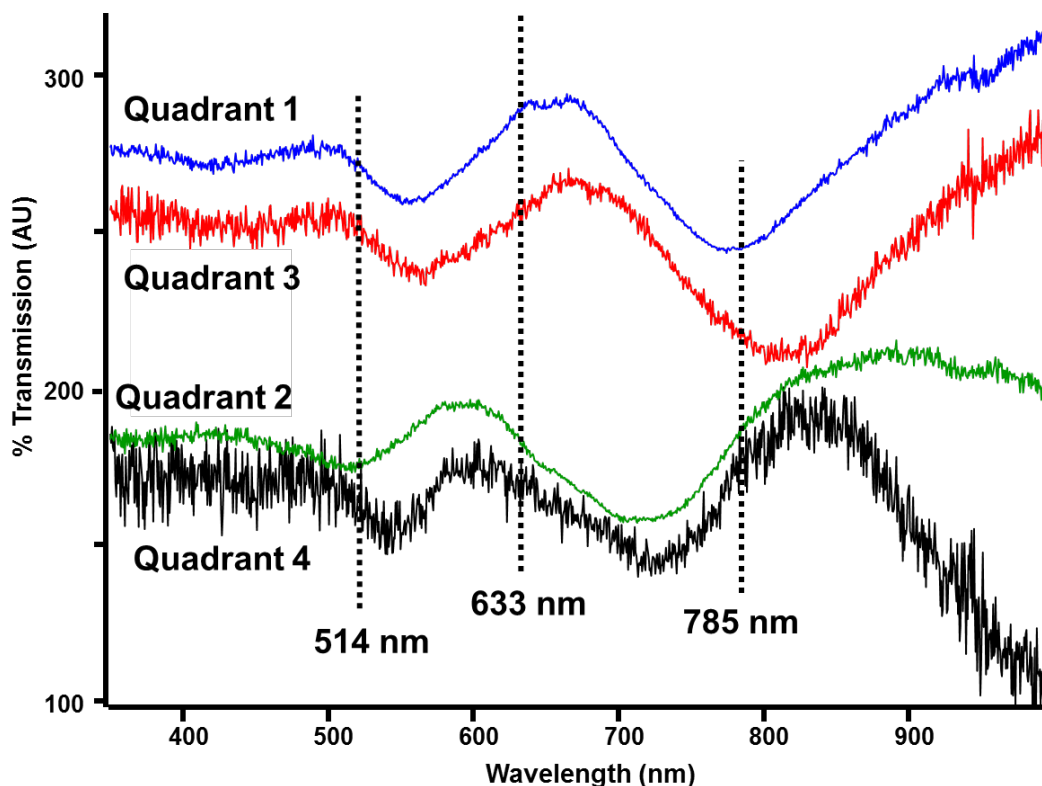


Fig. 7 ARL SERS substrate transmission data

Next the SERS signal response from the various quadrants of the ARL SERS substrate was measured and evaluated. In these experiments the well-characterized SERS active chemical BPE was used.¹³¹ BPE has main bands observed at 1200 cm^{-1} (assigned ethylenic C=C stretch band), 1588 cm^{-1} (assigned to the symmetric pyridyl ring breathing vibrational mode with coupled C–C stretching and C–H in-plane bending), and 1618 cm^{-1} (assigned to the stretching of the C=C double bond between the 2 pyridyl rings). Figure 8a shows an example of BPE/EtOH “typical” spectra. BPE is a hydrocarbon molecule that is structurally similar to pyridine (2 pyridine rings connected with a C=C double bond). It is widely used as a sensitive nonresonant spectroscopic probe for metal surfaces due to its large scattering cross section, conjugated Π -bond electrons, and 2 nitrogen atoms on the opposite sides of the molecule. Each nitrogen atom has a lone electron pair, which allows BPE to adsorb relatively strongly on metal surfaces. BPE adsorbs initially as a mixture of horizontal and vertical configurations. Then, at higher coverage values, the vertical configuration becomes dominant due to geometric constraints. Raman spectra exhibit 2 dominant bands at 1588 cm^{-1} and 1618 cm^{-1} for both metallic and oxidized Ag. The positions of these bands do not change with increasing BPE surface coverage, which with increasing BPE concentration in ethanol solutions has been previously observed via measured increases in the intensities of 1588 and 1618 cm^{-1} Raman bands.¹³¹ The intensities

of both bands increase, but the increases are not proportional. The ratio of the band intensities changes with increasing BPE concentrations. At low-BPE concentrations, the band at 1588 cm^{-1} is more prominent, and as the BPE concentration increases, the band at 1618 cm^{-1} becomes more prominent.

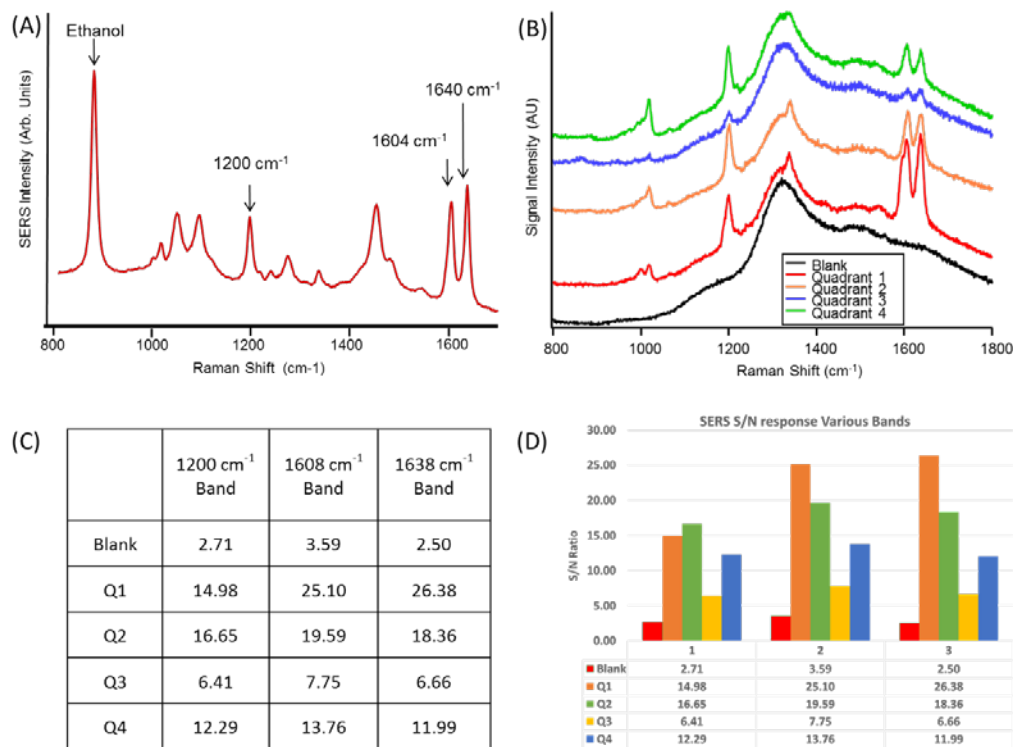


Fig. 8 a) Example SERS spectrum BPE, b) SERS of BPE on various quadrants of ARL SERS substrate, c) SNR for each quadrant at various bands, and d) data presented in graph format

For these experiments, BPE was dropped and dried ($2\ \mu\text{L}$) onto the SERS substrate surface and the resulting measurement collected. BPE was chosen as the probe in these experiments because of its high Raman scattering cross section, its ability to adsorb strongly and irreversibly to the Ag surface, and its lack of resonant enhancement in the visible region. The 1200-cm^{-1} peak of BPE was chosen for quantification because of its relative insensitivity to molecular orientation on an Ag surface. Figure 8b shows collected SERS data from various ARL SERS substrate quadrants. From data analysis on the signal-to-noise ratio for the 1200- , 1608- , and 1638-cm^{-1} bands, it appears that Quadrants 1 and 2 perform the best overall with largest overall numbers (Figs. 8c and 8d). Quadrant 2 performing as well as it did was surprising based on the plasmon absorbance data, but not if the spacing between the features is considered, which was most similar when comparing Quadrants 1 and 2. This likely allows for more features and “hot spots” across the substrate surface, which likely corresponds to an increase in overall enhancement.

4. Conclusions

An ARL SERS substrate for potential sensing and identification of unknown materials was demonstrated. We also demonstrated that the ARL SERS substrate was comparable to the previously available Klarite substrate. For future experiments, it would be valuable to consider a mask design with smaller and closer features, thus resulting in a significant increase in overall number/density of SERS hot spots across the substrate surface. Such a substrate surface might result in an overall more-“sensitive” SERS substrate capable of improving current SERS sensing capabilities for Army-relevant application.

5. References

1. Guicheteau JA, Hankus ME, Christesen SD, Emge D. Standard method for characterizing SERS substrates. Proceedings of SPIE Defense, Security, and Sensing Conference; 2012 Apr 23–27; Baltimore, MD. SPIE 8373.
2. Hankus M, Stratis-Cullum D, Pellegrino P. Enabling technologies for point and remote sensing of chemical and biological agents using Surface Enhanced Raman Scattering (SERS) techniques. Adelphi (MD): Army Research Laboratory (US); 2009. Report No.: ARL-TR-4957.
3. Hankus ME, Cullum BM. SERS nanoimaging probes for characterizing extracellular surfaces. Smart Biomedical and Physiological Sensor Technology V. 2007;6759:75908–75908.
4. Hankus ME, Li HG, Gibson GJ, Cullum BM. Surface-enhanced Raman scattering-based nanoprobe for high-resolution, non-scanning chemical imaging. Anal Chem. 2006;78:7535–7546.
5. Holthoff EL, Stratis-Cullum DN, Hankus ME. A nanosensor for TNT detection based on molecularly imprinted polymers and surface enhanced Raman scattering. Sensors. 2011;11:2700–2714.
6. Farrell ME, Holthoff EL, Pellegrino PM. Next generation Surface Enhanced Raman Scattering (SERS) substrates for Hazard Detection. Proceedings of the SPIE Defense, Security, and Sensing Conference; 2012 Apr 23–27; Baltimore, MD. SPIE 8358.
7. GarciaVidal FJ, Pendry JB. Collective theory for surface enhanced Raman scattering. Phys Rev Lett. 1996;77:1163–1166.
8. Kneipp J, Li X, Sherwood M, Panne U, Kneipp H, Stockman MI, Kneipp K. Gold nanolenses generated by laser ablation-efficient enhancing structure for surface enhanced Raman scattering analytics and sensing. Anal Chem. 2008;80:4247–4251.
9. K. Kneipp, H. Kneipp, R.R. Dasari, M.S. Feld. Single molecule Raman spectroscopy using silver and gold nanoparticles. Indian J Phys Proc Indian Assoc Cult Sci B. 2003;77B:39–47.
10. Li S, Li DW, Zhang QY, Tang X. Surface enhanced Raman scattering substrate with high-density hotspots fabricated by depositing Ag film on TiO₂-catalyzed Ag nanoparticles. J All Comp. 2016;689:439–445.

11. Liu YJ, Zhang ZY, Zhao Q, Zhao YP. Revisiting the separation dependent surface enhanced Raman scattering. *Applied Physics Letters*. 2008;93:3.
12. Otto A, Mrozek I, Grabhorn H, Akemann W. Surface enhanced Raman scattering. *J Phy-Cond Matt*. 1992;4:1143–1212.
13. Li ZY, Hattori HT, Parkinson P, Tian J, Fu L, Tan HH, Jagadish C. A plasmonic staircase nano-antenna device with strong electric field enhancement for surface enhanced Raman scattering (SERS) applications. *J Phys D-Appl Phys*. 2012;45.
14. Lu Y, Liu GL, Lee LP. High-density silver nanoparticle film with temperature-controllable interparticle spacing for a tunable surface enhanced Raman scattering substrate. *Nano Lett*. 2005;5:5–9.
15. Tian L, Tadepalli S, Farrell ME, Liu K-K, Gandra N, Pellegrino PM, Singamaneni S. Multiplexed charge-selective surface enhanced Raman scattering based on plasmonic calligraphy. *J Mat Chem*. 2014;C2:5438–5446.
16. Zhang C, Smirnov AI, Hahn D, Grebel H. Surface enhanced Raman scattering of biospecies on anodized aluminum oxide films. *Chem Phys Letters*. 2007;440:239–243.
17. Baker BE, Melville SM, Natan MJ. Combinatorially-optimized Ag-clad Au nanostructures for SERS. *ACS*. 1998;215:U74–U74.
18. Doering WE, Piotti ME, Natan MJ, Freeman RG. SERS as a foundation for nanoscale, optically detected biological labels. *Adv Mater*. 2007;19:3100.
19. Freeman RG et al. Self-assembled metal colloid monolayers – an approach to SERS substrates. *Science*. 1995;267(5204):1629–1632.
20. Freeman RG, Hommer MB, Grabar KC, Jackson MA, Natan MJ. Ag-clad Au nanoparticles: novel aggregation, optical, and surface-enhanced Raman scattering properties. *J Phys Chem*. 1996;100:718–724.
21. Grabar KC, Freeman RG, Hommer MB, Natan MJ. Preparation and characterization of Au colloid monolayers. *Anal Chem*. 1995;67:735–743.
22. Grabar KC, Smith PC, Musick MD, Davis JA, Walter DG, Jackson MA, Guthrie AP, Natan MJ. Kinetic control of interparticle spacing in Au colloid-based surfaces: rational nanometer-scale architecture. *ACS*. 1996;118(5):1148–1153.
23. He L, Mulvaney SP, St Angelo SK, Natan MJ. New SERS-active substrates based on thin films of noble metals. *ACS*. 1998;216:U631–U631.

24. Mulvaney SP, Musick MD, Keating CD, Natan MJ. Glass-coated, analyte-tagged nanoparticles: a new tagging system based on detection with surface-enhanced Raman scattering. *Langmuir*. 2003;19:4784.
25. Mulvaney SP, Musick MD, Keating CD, Natan MJ, Glass C. A new tagging system based on detection with surface-enhanced Raman scattering. *Langmuir*. 2003;19:4784.
26. Banchelli M, Tiribilli B, Pini R, Dei L, Matteini P, Caminati G. Controlled graphene oxide assembly on silver nanocube monolayers for SERS detection: dependence on nanocube packing procedure. *Beilstein J of Nanotech*. 2016;7:9–21.
27. Mahmoud MA. Super-radiant plasmon mode is more efficient for SERS than the sub-radiant mode in highly packed 2D gold nanocube arrays. *J Chem Phys*. 2015;143.
28. Liu M, Wang Z, Zong S, Zhang R, Shu D, Xu S, Wang C, Cui Y. SERS-based DNA detection in aqueous solutions using oligonucleotide-modified Ag nanoprisms and gold nanoparticles. *Anal and Bioanal Chem*. 2013;405(18):6131–6136.
29. Feng C, Zhao Y, Jiang Y. Interesting polarization-independent SERS detection performance induced by the rotation symmetry of multiparticle nanostructures. *Nanotech*. 2016;27.
30. Gao Y, Li Y, Chen J, Zhu S, Liu X, Zhou L, Shi P, Niu D, Gu J, Shi J. Multifunctional gold nanostar-based nanocomposite: synthesis and application for noninvasive MR-SERS imaging-guided photothermal ablation. *Biomaterials*. 2015;60:31–41.
31. Li A, Tang L, Song S, Ma W, Xu L, Kuang H, Wu X, Liu L, Chen X, Xu C. A SERS-active sensor based on heterogeneous gold nanostar core-silver nanoparticle satellite assemblies for ultrasensitive detection of aflatoxinB1. *Nanoscale*. 2016;8(4):1873–1878.
32. Bai XL, Xu SY, Hu GF, Wang LY. Surface plasmon resonance-enhanced photothermal nanosensor for sensitive and selective visual detection of 2,4,6-trinitrotoluene. *Sens Act B-Chem*. 2016;237:224–229.
33. Cao XW, Shi C, Lu W, Zhao H, Wang M, Zhang M, Chen X, Dong J, Han X, Qian W. Surface enhanced Raman scattering probes based on antibody conjugated Au nanostars for distinguishing lung cancer cells from normal cells. *J Nanosci Nanotech*. 2016;16(12):12161–12171.

34. Li JL, Sun DW, Pu HB, Jayas DS. Determination of trace thiophanate-methyl and its metabolite carbendazim with teratogenic risk in red bell pepper (*Capsicum annuum* L.) by surface-enhanced Raman imaging technique. *Food Chem.* 2017;218:543–552.
35. Reymond-Laruinaz S, Saviot L, Potin V, de Lucas MDM. Protein-nanoparticle interaction in bioconjugated silver nanoparticles: a transmission electron microscopy and surface enhanced Raman spectroscopy study. *Appl Sur Sci.* 2016;389:17–24.
36. Dieringer JA, McFarland AD, Shah NC, Stuart DA, Whitney AV, Yonzon CR, Young MA, Zhang X, Van Duyne RP. Surface enhanced Raman spectroscopy: new materials, concepts, characterization tools, and applications. *Faraday Discuss.* 2006;132:9–26.
37. Shafer-Peltier KE, Haynes CL, Glucksberg MR, Van Duyne RP. Toward a glucose biosensor based on surface-enhanced Raman scattering. *ACS.* 2003;125:588–593.
38. Stewart ME, Anderton CR, Thompson LB, Maria J, Gray SK, Rogers JA, Nuzzo RG. Nanostructured plasmonic sensors. *Chem Rev* 2008;108(2):494–521.
39. Willets KA, Van Duyne RP. Localized surface plasmon resonance spectroscopy and sensing. *Annl Rev Phys Chem.* 2007;58:267–297.
40. Botti S, Ruffoloni A, Laurenzi S, Gay S, Rindzevicius T, Schmidt MS, Santonicola MG. DNA self-assembly on graphene surface studied by SERS mapping. *Carbon.* 2016;109:363–372.
41. Focsan M, Campu A, Craciun AM, Potara M, Leordean C, Maniu D, Astilean S. A simple and efficient design to improve the detection of biotin-streptavidin interaction with plasmonic nanobiosensors. *Biosens Bioelect.* 2016;86:728–735.
42. Li JJ, An HQ, Zhu J, Zhao JW. Detecting glucose by using the Raman scattering of oxidized ascorbic acid: the effect of graphene oxide-gold nanorod hybrid. *Sens Act B-Chem.* 2016;235:663–669.
43. Nguyen AH, Shin Y, Sim SJ. Development of SERS substrate using phage-based magnetic template for triplex assay in sepsis diagnosis. *Biosens Bioelect.* 2016;85:522–528.

44. Qi GH, Wang Y, Zhang B, Sun D, Fu C, Xu W, Xu S. Glucose oxidase probe as a surface-enhanced Raman scattering sensor for glucose. *Anal Bioanal Chem.* 2016;408(26):7513–7520.
45. Hirsch LR, Gobin AM, Lowery AR, Tam F, Drezek RA, Halas NJ, West JL. Metal nanoshells. *Ann Biomed Eng.* 2006;34(1):15–22.
46. Huang J, Zong C, Shen H, Liu M, Chen B, Ren B, Zhang Z. Mechanism of cellular uptake of graphene oxide studied by surface-enhanced Raman spectroscopy. *Small.* 2012;8(16):2577–2584.
47. Qian J, Jiang L, Cai FH, Wang D, He SL. Fluorescence-surface enhanced Raman scattering co-functionalized gold nanorods as near-infrared probes for purely optical in vivo imaging. *Biomaterials.* 2011;32:1601–1610.
48. Qian XM, Peng XH, Ansari DO, Yin-Goen Q, Chen GZ, Shin DM, Yang L, Young AN, Wang MD, Nie S. In vivo tumor targeting and spectroscopic detection with surface-enhanced Raman nanoparticle tags. *Nat Biotech.* 2008;26(1):83–90.
49. Sanles-Sobrido M, Exner W, Rodriguez-Lorenzo L, Rodriguez-Gonzalez B, Correa-Duarte MA, Alvarez-Puebla RA, Liz-Marzan LM. Design of SERS-encoded, submicron, hollow particles through confined growth of encapsulated metal nanoparticles. *ACS.* 2009;131(7):2699–2705.
50. Song JB, Zhou JJ, Duan HW. Self-assembled plasmonic vesicles of SERS-encoded amphiphilic gold nanoparticles for cancer cell targeting and traceable intracellular drug delivery. *ACS.* 2012;134:13458–13469.
51. Vendrell M, Maiti KK, Dhaliwal K, Chang YT. Surface-enhanced Raman scattering in cancer detection and imaging. *Trend Biotech.* 2013;31:249–257.
52. Wang XJ, Wang C, Cheng L, Lee ST, Liu Z. Noble metal coated single-walled carbon nanotubes for applications in surface enhanced Raman scattering imaging and photothermal therapy. *ACS.* 2012;134:7414–7422.
53. Wang ZY, Zong SF, Yang J, Li J, Cui YP. Dual-mode probe based on mesoporous silica coated gold nanorods for targeting cancer cells. *Biosens Bioelect.* 2011;26:2883–2889.
54. Yang M, Alvarez-Puebla R, Kim H-S, Aldeanueva-Potel P, Liz-Marzan LM, Kotov NA. SERS-active gold lace nanoshells with built-in hotspots. *Nano Lett.* 2010;10(10):4013–4019.
55. Liu, SH, Han MY. Silica-coated metal nanoparticles. *Chem.* 2010;5:36–45.

56. Lu WT, Singh AK, Khan SA, Senapati D, Yu H, Ray PC. Gold nano-popcorn-based targeted diagnosis, nanotherapy treatment, and in situ monitoring of photothermal therapy response of prostate cancer cells using surface-enhanced Raman spectroscopy. *ACS*. 2010;132(51):18103–18114.
57. Schwartzberg AM, Zhang JZ. Novel optical properties and emerging applications of metal nanostructures. *J Phys Chem C*. 2008;112:10323–10337.
58. von Maltzahn G, Centrone A, Park J-H, Ramanathan R, Sailor MJ, Hatton TA, Bhatia SN. SERS-coded gold nanorods as a multifunctional platform for densely multiplexed near-infrared imaging and photothermal heating. *Adv Mat*. 2009;21:3175–3180.
59. Zhang JZ, Noguez C. Plasmonic optical properties and applications of metal nanostructures. *Plasm*. 2008;3:127–150.
60. Jones JP, Fell NF, Alexander T, Fountain AW. Photonic nanostructures as SERS substrates for reproducible characterization of bacterial spores. *SPIE*. 2004;5416:94–104.
61. Kneipp H, Kneipp K. Surface-enhanced hyper Raman scattering in silver colloidal solutions. *J Ram Spectros*. 2005;36:551–554.
62. Kao P, Malvadkar NA, Cetinkaya M, Wang H, Allara DL, Demirel MC. Surface-enhanced Raman detection on metalized nanostructured poly(p-xylylene) films. *Adv Mat*. 2008;20(18):3562–3565.
63. Kho KW, Shen ZX, Zeng HC, Soo KC, Olivo M. Deposition method for preparing SERS-active gold nanoparticle substrates. *Anal Chem*. 2005;77:7462–7471.
64. Farrell ME, Strobbia P, Sarkes DA, Stratis-Cullum DN, Cullum BM, Pellegrino PM. The development of Army relevant peptide-based surface enhanced Raman scattering (SERS) sensors for biological threat detection. *SPIE*. 2016;9863.
65. Li H, Baum CE, Cullum BM. Characterization of novel gold SERS substrates with multilayer enhancements. *SPIE*. 2006;6380.
66. Li H, Baum CE, Sun J, Cullum BM. Multilayer enhanced SERS active materials: fabrication, characterization, and application to trace chemical detection. *SPIE*. 2006;6218:621804.
67. Li H, Patel PH, Cullum BM. Novel multilayered SERS substrates for trace chemical and biochemical analysis. *SPIE*. 2004;5588.

68. Strobbia P, Henegar A, Gougousi T, Cullum BM. Characterization of the role of oxide spacers in multilayer-enhanced SERS probes. *SPIE*. 2015;9487.
69. Dick LA, McFarland AD, Haynes CL, Van Duyne RP. Metal film over nanosphere (MFON) electrodes for surface-enhanced Raman spectroscopy (SERS): improvements in surface nanostructure stability and suppression of irreversible loss. *J Phys Chem B*. 2002;106:853–860.
70. Sharma B, Frontiera RR, Henry AI, Ringe E, Van Duyne RP. SERS: materials, applications, and the future. *Mater Today*. 2012;15:16–25.
71. Hankus ME, Stratis-Cullum DN, Pellegrino PM. Characterization of next-generation commercial surface-enhanced Raman scattering (SERS) substrates. *SPIE*. 2011;8018.
72. Klutse CK, Cullum BM. Development of SAM-based multi-layer SERS substrates for intracellular analyses. *SPIE*. 2010;7674.
73. Klutse CK, Cullum BM. Optimization of SAM-based multilayer SERS substrates for intracellular analyses: the effect of terminating functional groups. *SPIE*. 2011;8025.
74. Li HG, Baum CE, Cullum BM. Characterization of novel gold SERS substrates with multilayer enhancements. *SPIE*. 2006;6380.
75. Li HG, Baum CE, Sun J, Cullum BM. Multilayer enhanced SERS active materials: fabrication, characterization, and application to trace chemical detection. *SPIE*. 2006;6218:21804–21804.
76. Li HG, Patel PH, Cullum BM. Novel multilayered SERS substrates for trace chemical and biochemical analysis. *SPIE*. 2004;5588:87–97.
77. Akin MS, Yilmaz M, Babur E, Ozdemir B, Erdogan H, Tamer U, Demirel G. Large area uniform deposition of silver nanoparticles through bio-inspired polydopamine coating on silicon nanowire arrays for practical SERS applications. *J Mat Chem B*. 2014;2:4894–4900.
78. Baniukevic J, Hakki BI, Goktug BA, Tamer U, Ramanavicius A, Ramanaviciene A. Magnetic gold nanoparticles in SERS-based sandwich immunoassay for antigen detection by well oriented antibodies. *Biosens Bioelect*. 2013;43:281–288.
79. Braun G, Pavel I, Morrill AR, Seferos DS, Bazan GC, Reich NO, Moskovits M. Chemically patterned microspheres for controlled nanoparticle assembly in the construction of SERS hot spots. *J Am Chem Soc*. 2007;129(25):7760–7761.

80. David C, Guillot N, Shen H, Toury T, de la Chapelle ML. SERS detection of biomolecules using lithographed nanoparticles towards a reproducible SERS biosensor. *Nanotech.* 2010;21.
81. Gopinath A, Boriskina SV, Reinhard BM, Dal Negro L. Deterministic aperiodic arrays of metal nanoparticles for surface-enhanced Raman scattering (SERS). *Opt Exp.* 2009;17:3741–3753.
82. Guven B, Basaran-Akgul N, Temur E, Tamer U, Boyaci IH. SERS-based sandwich immunoassay using antibody coated magnetic nanoparticles for *Escherichia coli* enumeration. *Analyst.* 2011;136:740–748.
83. Kumar GVP. Gold nanoparticle-coated biomaterial as SERS micro-probes. *Biosens Bioelect.* 2011;34:417–422.
84. Li J-M, Ma W-F, Wei C, Guo J, Hu J, Wang C-C. Poly(styrene-co-acrylic acid) core and silver nanoparticle/silica shell composite microspheres as high performance surface-enhanced Raman spectroscopy (SERS) substrate and molecular barcode label. *J Mat Chem B.* 2011;21:5992–5998.
85. Qian XM, Nie SM. Single-molecule and single-nanoparticle SERS: from fundamental mechanisms to biomedical applications. *Chem Soc Rev.* 2008;37:912–920.
86. Tanahashi I, Harada Y. Naturally inspired SERS substrates fabricated by photocatalytically depositing silver nanoparticles on cicada wings. *Nano Res Lett.* 2014;9:298–302.
87. Tanahashi I, Harada Y. Silver nanoparticles deposited on TiO₂-coated cicada and butterfly wings as naturally inspired SERS substrates. *J Mat Chem C.* 2015;3:5721–5726.
88. Theiss J, Pavaskar P, Echternach PM, Muller RE, Cronin SB. Plasmonic nanoparticle arrays with nanometer separation for high-performance SERS substrates. *Nano Lett.* 2010;10:2749–2754.
89. Novara C, Petracca F, Virga A, Rivolo P, Ferrero S, Chiolerio A, Geobaldo F, Porro S, Giorgis F. SERS active Ag nanoparticles in mesoporous silicon: detection of organic molecules and peptide-antibody assays. *J Ram Spectros.* 2012;43:730–736.
90. Im H, Bantz KC, Lindquist NC, Haynes CL, Oh SH. Vertically oriented sub-10-nm plasmonic nanogap arrays. *Nano Lett.* 2010;10:2231–2236.

91. Sawai Y, Takimoto B, Nabika H, Ajito K, Murakoshi K. Observation of a small number of molecules at a metal nanogap arrayed on a solid surface using surface-enhanced Raman scattering. *ACS*. 2007;129:1658–1662.
92. Jian Z, Irannejad M, Bo C. Bowtie nanoantenna with single-digit nanometer gap for surface-enhanced Raman scattering (SERS). *Plasmonics*. 2015;10:831–837.
93. Peters RF, Gutierrez-Rivera L, Dew SK, Stepanova M. Surface enhanced Raman spectroscopy detection of biomolecules using EBL fabricated nanostructured substrates. *J Vis Exp*. 2015;97:52712.
94. Borys NJ, Lupton JM. Surface-enhanced light emission from single hot spots in Tollens reaction silver nanoparticle films: linear versus nonlinear optical excitation. *J Phys Chem C*. 2011;115:13645–13659.
95. Chang H-W, Tsai Y-C, Cheng C-W, Lin C-Y, Lin Y-W, Wu T-M. Nanostructured Ag surface fabricated by femtosecond laser for surface-enhanced Raman scattering. *J Coll Interf Sci*. 2011;360(1):305–308.
96. Huo HB, Wang C, Ren HZ, Johnson M, Shen MY. Surface enhanced Raman scattering sensing with nanostructures fabricated by soft nanolithography. *J Macromolec Sci A - Pure Appl Chem*. 2009;46:1182–1184.
97. Wang C, Chang Y-C, Yao J, Luo C, Yin S. Surface enhanced Raman spectroscopy by interfered femtosecond laser created nanostructures. *Appl Phys Lett*. 2012;100.
98. Xu B-B et al. Surface-plasmon-mediated programmable optical nanofabrication of an oriented silver nanoplate. *ACS Nano*. 2014;8(7):6682–6692.
99. Xu W, Ling X, Xiao J, Dresselhaus MS, Kong J, Xu H, Liu Z, Zhang J. Surface enhanced Raman spectroscopy on a flat graphene surface. *PNAS*. 2012;109:9281–9286.
100. Das G, Patra N, Gopalakrishnan A, Zaccaria RP, Toma A, Thorat S, DiFabrizio E, Diaspro A, Salerno M. Fabrication of large-area ordered and reproducible nanostructures for SERS biosensor application. *Analyst*. 2012;137:1785–1792.
101. Lu X, Samuelson DR, Xu Y, Zhang H, Wang S, Rasco BA, Xu J, Konkel ME. Detecting and tracking nosocomial methicillin-resistant staphylococcus aureus using a microfluidic SERS biosensor. *Anal Chem*. 2013;85(4):2320–2327.

102. Srivastava SK, Shalabney A, Khalaila I, Gruner C, Rauschenbach B, Abdulhalim I. SERS biosensor using metallic nano-sculptured thin films for the detection of endocrine disrupting compound biomarker vitellogenin. *Small*. 2014;10(17):3579–3587.
103. Arslanoglu J, Zaleski S, Loike J. An improved method of protein localization in artworks through SERS nanotag-complexed antibodies. *Anal Bioanal Chem*. 2011;399:2997–3010.
104. Das G, Mecarini F, Gentile F, DeAngelis F, Kumar HGM, Candeloro P, Liberale C, Cuda G, DiFabrizio E. Nano-patterned SERS substrate: application for protein analysis vs. temperature. *Biosens Bioelect*. 2009;24:1693–1699.
105. Fabris L, Dante M, Nguyen TQ, Tok JBH, Bazan GC. SERS aptatags: new responsive metallic nanostructures for heterogeneous protein detection by surface enhanced Raman spectroscopy. *Adv Funct Mater*. 2008;18:2518–2525.
106. Kim J-H et al. Nanoparticle probes with surface enhanced Raman spectroscopic tags for cellular cancer targeting. *Anal Chem*. 2006;78(19):6967.
107. Botti S, Cantarini L, Almaviva S, Puiu A, Rufoloni A. Assessment of SERS activity and enhancement factors for highly sensitive gold coated substrates probed with explosive molecules. *Chem Phys Lett*. 2014;592:277–281.
108. Efrima S, Zeiri L. Understanding SERS of bacteria. *J Raman Spect*. 2009;40:277–288.
109. Guzelian AA, Sylvia JM, Janii JA, Clauson SL, Spencer KM. SERS of whole bacteria and trace levels of biological molecules. *SPIE*. 2002;4577:182–192.
110. Jarvis RM, Goodacre R. Characterisation and identification of bacteria using SERS. *Chem Soc Rev*. 2008;37:931–936.
111. Jian S, Hankus ME, Cullum BM. SERS based immuno-microwell arrays for multiplexed detection of foodborne pathogenic bacteria. *SPIE*. 2009;7313:73130.
112. Liu YL, Chen Y-R, Nou XW, Kim MS, Chao KL. Label-free SERS for rapid species identification of escherichia coli, listeria monocytogenes, and salmonella typhimurium bacteria. *Spectroscopy*. 2008;23(2):48–54.
113. Patel IS, Premasiri WR, Moir DT, Ziegler LD. Barcoding bacterial cells: a SERS-based methodology for pathogen identification. *J Raman Spect*. 2008;39:1660–1672.

114. Premasiri WR, Moir DT, Klempner MS, Krieger N, Jones II G, Ziegler LD. Characterization of the surface enhanced Raman scattering (SERS) of bacteria. *J Phys Chem B*. 2005;109(1):312–320.
115. Gupta VK, Atar N, Yola ML, Eryilmaz M, Torul H, Tamer U, Boyaci IH, Ustundag Z. A novel glucose biosensor platform based on Ag@AuNPs modified graphene oxide nanocomposite and SERS application. *J Coll Interf Sci*. 2013;406:231–237.
116. Park H, Lee S, Chen L, Lee EK, Shin SY, Lee YH, Son SW, Oh CH, Song JM, Kang SH, Choo J. SERS imaging of HER2-overexpressed MCF7 cells using antibody-conjugated gold nanorods. *Phys Chem Chem Phys*. 2009;11(34):7444–7449.
117. Farquharson S, Shende C, Smith W, Huang H, Inscore F, Sengupta A, Sperry J, Sickler T, Prugh A, Guicheteau J. Selective detection of 1000 B. anthracis spores within 15 minutes using a peptide functionalized SERS assay. *Analyst*. 2014;139:6366–6370.
118. Nergiz SZ, Gandra N, Farrell ME, Tian L, Pellegrino PM, Singamaneni S. Biomimetic SERS substrate: peptide recognition elements for highly selective chemical detection in chemically complex media. *J Mat Chem A*. 2013;1:6543–6549.
119. Wei F, Zhang D, Halas NJ, Hartgerink JD. Aromatic amino acids providing characteristic motifs in the Raman and SERS spectroscopy of peptides. *J Phys Chem B*. 2008;112:9158–9164.
120. Jing C, Qin G, Chen Q, Yu J, Li S, Cao F, Yang B, Ren Y. Synergistic combination of diatomaceous earth with Au nanoparticles as a periodically ordered, button-like substrate for SERS analysis of the chemical composition of eccrine sweat in latent fingerprints. *J Mat Chem C*. 2015;3:4933–4944.
121. Kroeger N, Brunner E. Complex-shaped microbial biominerals for nanotechnology. *Wiley Inter Rev - Nanomed Nanobiotech*. 2014;6:615–627.
122. Sun Yong K, Sehyun P, Nichols WT. Self-assembled diatom substrates with plasmonic functionality. *ACS*. 2014;64:1179–1184.
123. Yang J, Rorrer GL, Wang AX. Bioenabled SERS substrates for food safety and drinking water monitoring. *SPIE*. 2015;9488.
124. Yang J, Zhen L, Ren F, Campbell J, Rorrer GL, Wang AX. Ultra-sensitive immunoassay biosensors using hybrid plasmonic-biosilica nanostructured materials. *J Biophot*. 2015;8:659–667.

125. Daglar B, Demirel GB, Khudiyev T, Dogan T, Tobail O, Altuntas S, Buyukserin F, Bayindir M. Anemone-like nanostructures for non-lithographic, reproducible, large-area, and ultra-sensitive SERS substrates. *Nano*. 2014;6(21):12710–12717.
126. Chou S-Y, Yu C-C, Yen Y-T, Lin K-T, Chen H-L, Su W-F. Romantic story or Raman scattering? Rose petals as ecofriendly, low-cost substrates for ultrasensitive surface-enhanced Raman scattering. *Anal Chem*. 2015;87:6017–6024.
127. Zhou Q, Meng G, Wu N, Zhou N, Chen B, Li F, Huang Q. Dipping into a drink: basil-seed supported silver nanoparticles as surface-enhanced Raman scattering substrates for toxic molecule detection. *Sens Act B - Chem*. 2016;223:447–452.
128. Luna C, Chavez VH, Diaz Barriga-Castro E, Nunez NO, Mendoza-Resendez R. Biosynthesis of silver fine particles and particles decorated with nanoparticles using the extract of *Illicium verum* (star anise) seeds. *Spectrochimica Acta Part A - Mol Biomol Spectros*. 2015;141:43–50.
129. Hankus ME, Stratis-Cullum DN, Pellegrino PM. Surface enhanced Raman scattering (SERS)-based next generation commercially available substrate: physical characterization and biological application. *SPIE*. 2011;8099.
130. Lee CH, Hankus ME, Tian L, Pellegrino PM, Singamaneni S. Plasmonic paper as a highly efficient SERS substrate. *SPIE*. 2012;8358.
131. Guicheteau JA, Farrell ME, Christesen SD, Fountain AW, Pellegrino PM, Emmons ED, Tripathi A, Wilcox P, Emge D. Surface-enhanced Raman scattering (SERS) evaluation protocol for nanometallic surfaces. *Appl Spectros*. 2013;67:396–403.
132. Alexander TA. Applications of surface-enhanced Raman spectroscopy (SERS) for biosensing: an analysis of reproducible, commercially available substrates. *SPIE*. 2005;6007:600703.
133. Alexander TA. Development of methodology based on commercialized SERS-active substrates for rapid discrimination of poxviridae virions. *Anal Chem*. 2008;80:2817–2825.
134. Alexander TA, Le DM. Characterization of a commercialized SERS-active substrate and its application to the identification of intact bacillus endospores. *Appl Opt*. 2007;46.

135. Alexander TA, Pellegrino PM, Gillespie JB. Near-infrared surface-enhanced-Raman-scattering-mediated detection of single optically trapped bacterial spores. *Appl Spectros.* 2003;57:1340–1345.
136. Netti MC, Zoorob ME, Charlton MD, Ayliffe P, Mahnkopf S, Stopford P, Todd K, Lincoln JR, Perney NMB, Baumberg JJ. Probing molecules by surface-enhanced Raman spectroscopy. *SPIE.* 2006;60937.
137. CI AZ 5214 E image reversal photoresist [accessed 2017 Sep 21]. <http://dvh.physics.illinois.edu/pdf/AZ5214E.pdf>.

INTENTIONALLY LEFT BLANK.

Appendix. Supplemental Information

This appendix appears in its original form, without editorial change.

Approved for public release; distribution is unlimited.

Plasma Therm 790+ Oxide/nitride PECVD (silicon nitride deposition)

Target thickness: 100 nm of silicon nitride, deposited at a rate of 12.01nm/min, ~10min needed.

- 1) Make sure the power is on
- 2) In the software, select Process (“Justin SiNx”) recipe
- 3) Set recipe temperature
- 4) Vent Chamber
- 5) Pump chamber and wait for temperature to achieve set point
- 6) Input job ID
- 7) Start job, process time, start job
- 8) Alarm sounds when process complete

*If deposited a lot of material, be sure to run a clean recipe

Nanometrics NanoSpec 3000 PHV

- 1) Use the nitride on Si option
- 2) Turn on
- 3) Calibrate
- 4) Dark- angle, bare- reflectance
- 5) measure

EVG 120 Resist Processing Cluster

- Mask with acetone, IPA and water cleaner (mask side up)

EVG 120 Resist Processing Center

- 1) This is an HMDS-adhesion promotor, photoresist AZ 5214E, when loading wafer keep the major flat on top
- 2) Click cassette
- 3) Tilt cassette

Click cassette, start

Recipe 4CAZ5214E_4KA_110C

Select slot 1

OK

Hot plate- Brewer Science

- 1) GD Bake 110°C for 1 minute = recipe
- 2) Load
- 3) Select Process

Karl Suss MA6/BA6 Contact aligner

- 1) Measure the Dose from the lamp
- 2) Change the mask
- 3) Lamp test, ~8.5MW/cm
- 4) Lamp test off, 60mJ/cm~7sec
- 5) Select program – hand or Val
- 6) Edit Program, exp time=7 sec
- 7) Change mask, want pattern CR side up
- 8) Enter
- 9) Load into holder, move rotational always set at 0
- 10) Load, check wafer shiny side up
- 11) Enter, move slide in
- 12) Enter
- 13) Exposure
- 14) Change mask
- 15) Enter- to turn off mask vacuum

Hotplate

- 2 minutes at 120°C recipe

Karl suss- Flood exposure

- 1) Select program, change mask

- 2) Enter
- 3) Flood-E
- 4) Select program
- 5) Edit parameter ~30sec, edit parameter
- 6) Load, after complete move parameter off Flood-E because can impact next user

TAM H Developer (Hood 11)- exposure development

- 1) Place wafer in AZ 300 MIF (2%) for 30 sec,
- 2) Wash wafer in water
- 3) Dry
- 4) Characterize wafer with microscope using yellow filter

MetroLine M4L

- 1) This is used to remove any debris from the wafer
- 2) Should be in hibernate mode, will click to stop pump
- 3) Open door (latch doesn't work, need to flip up latch)
- 4) Use 2nd slot with contents toward back
- 5) Place wafer in, active side up in center
- 6) Recipe- 5214 descum 2 minutes
- 7) Run, input name
- 8) This can take a while to pump down

Unaxis ULR 700 Etch PM 3 (nitride etch)

- 1) Typically you want to do a ½ etch, measure and then calculate the rest of the etch, add ~15-20% more time for the etch. For these substrates, we calculated that the etch rate was 3.25 nm/sec, requiring a 20 sec etch time.
- 2) Editors
 1. Flow- robot arm directions
 2. Sequence-what steps to do

3. Edit Steps- allows the user to change the sequence of steps. Usually only process time is changed.
4. *note the flow rate is important with pressure
- 3) Vent/Lock- load wafer (open door) use cassette #2 (slot 1=sample, slot 2=dummy)
- 4) Load 2 wafers, the sample and dummy. Vent button will turn yellow and a soft beep will be heard.
- 5) Pump Lock
- 6) Lot Operators- name, slot, flow, ADD, cassette select and execute
- 7) Vent Lock
- 8) Measure substrate with Nanometrics NanoSpec 3000 PHV
- 9) After measurement and determination of etch rate, need to complete etch. Click on PM3, select SINCF4/CH3 condition
- 10) Keg O2 clean – edit step, process time can be changed, usually 600 sec
- 11) Keg SiN Etch CF4_CHF3, process time 2 minutes
- 12) SAVE step
- 13) Return
- 14) Select 1st Editors, lot operation, lot ID_.1
- 15) Flow PM3-keg_SiNcF4_CHF3
- 16) Add1, que material
- 17) Select cassette #2, execute
- 18) Module status allows you to watch the process occurring.
- 19) Complete this process for the dummy and then the sample wafer

IPA/acetone clean

- 1) Use two large clean dishes
- 2) Acetone 5 min, fresh acetone 5 min, IPA 5 min

Piranha Photoresist Strip

- 1) PPO includes gloves and goggles
- 2) Always use Teflon tweezers when working with Piranha solution

- 3) Samples need to first be wetted in water bath
- 4) Combine peroxide (1/2 total amount) with sulfuric acid, slowly. Then add rest of peroxide to sulfuric acid (in large petri dish)
- 5) Look for bubbles on surface of wafer= cleaning off photoresist and any organic contaminants
- 6) Assume 20 minutes is enough for a good clean
- 7) Rinse by putting wafer into large petri dish of water, dry with air hose, use metal tweezers and water from faucet.

KOH Etch

- 1) Waste goes in container under the hood
- 2) Always use the same temperature, 80°C when etching, 45% w/w/ solution KOH (already made and provided in cleanroom)
- 3) PPE: gloves, shield, apron
- 4) Use metal tweezers
- 5) KOH, need 3/4 inch in the large petri dish
- 6) Set thermocouple to 80°C
- 7) With remaining probe, turn device temp off to prevent temp rising when probe is removed and it does not register a solution)
- 8) This takes about 5 min, will see lots of bubbles
- 9) Wet wafer surface with water before placing into KOH bath
- 10) Measure etch with Leica microscope

HCL clean

- 1) The purpose of this clean is to remove the KOH precipitate from the etch
- 2) You will need to add 200 mL of water to 50 mL of HCL, wash 5 minutes
- 3) Then insert wafer into a water bath

HF etch (49%, premade solution)

- 1) This is used to remove the nitride mask layer
- 2) Proper PPE includes gloves, face mask and apron

- 3) Only use Teflon/plastic containers (no glass)
- 4) Wet the surface of the wafer with water, then insert into the HF bath for 3 min. you should see a color change and the etch occurs, swish solution occasionally
- 5) Wash in water. The surface should now be extremely hydrophobic
- 6) Repeat water wash step 2x, blow dry wafer

CHA Evaporator

- 1) Pump down the process
- 2) Turn off the high voltage (panel controller-1)
- 3) Pump control (panel Tech II)
 - Automatic
 - Switch to vent- will vent chamber and lift the lid
- 4) Fixture control panel
 - Turn switch to open
 - Check for delamination of shutter, remove any debris with razor blade, vacuum up flakes to prevent any possible contamination
- 5) Gun Rotation Panel
 - Manual
 - Knobs to crucible (Cr)
 - Cr crucible needs to be inserted, ensure that any material added to it does not stick out and instead is level.
 - CRU3- This is the Au crucible to be inserted (always insure that switch is OFF when inserting hands into the machine)
 - When done, move switch back to Auto
- 6) Fixture Control Panel
 - Close shutter, move to Auto
- 7) Auto Tech II panel
 - Knob to automatic
 - Knob to start and lower – will lower dome and automatically start the pump down process (will hear distinct noises associated with this process)

- 8) Fixture Control Panel
 - Auto Rotation on – will allow escape of any gasses
- 9) Vacuum Gauge Controller
 - IG1- turn on
 - IG2-turn on, for deposition want $7.5 \text{ E-}7$ Torr

SEM

- 1) Turn pump off
- 2) Purge- takes a few seconds, load sample onto holder, screw in place, lift latch 1
- 3) Pump, hear it start, proceed will turn green
- 4) Close
- 5) Open, push sample stage back in (up position), will feel some resistance, unscrew platform, pull out, restore latch 2
- 6) Open- dark
- 7) Close- light
- 8) Close the doors to the outside panel
- 9) In the software, hit the resume button on the keyboard, 10 sec delay [resume completed] OK
- 10) [EHT] click, EHT on (this turns on the gun)
- 11) Bring the sample to within 10mm of the sample (1 inch proximity)
- 12) Gun Tab EHT=3.5KV
- 13) Detector Tab, Signal A, InLEns is most commonly used
- 14) Scanning Tab use continuous avg when looking for feature,
- 15) Collect images
- 16) When done collecting images, turn EHT off, drop stage, hit [exchange] on keyboard.
- 17) Follow removal process by repeating steps 1-8 in reverse order.
- 18) Leave doors to SEM open

List of Symbols, Abbreviations, and Acronyms

2-D	2-dimensional
3-D	3-dimensional
AFM	atomic force microscopy
Ag	silver
ARL	US Army Research Laboratory
Au	gold
BA	benzoic acid
BPE	trans-1,2-bis(4-pyridyl)-ethylene
Cr	chromium
EBL	electron beam lithography
ECBC	Edgewood Chemical Biological Center
EM	electromagnetic
FONs	film over nanoparticles
HCl	hydrogen chloride
HF	hydrofluoric acid
HMDS	hexamethyldisilazane
IPA	isopropyl alcohol
KOH	potassium hydroxide
PECVD	plasma-enhanced chemical vapor deposition
PETN	pentaerythritol tetranitrate
RDX	1,3,5-trinitroperhydro-1,3,5-triazine
RSD	relative standard deviation
SEM	scanning electron microscopy
SERS	Surface Enhanced Raman Scattering
SiN	silicon nitride
SPR	surface plasmon resonance
TMAH	tetra methyl ammonium hydroxide
TNT	trinitrotoluene

1 DEFENSE TECHNICAL
(PDF) INFORMATION CTR
DTIC OCA

2 DIR ARL
(PDF) IMAL HRA
RECORDS MGMT
RDRL DCL
TECH LIB

1 GOVT PRINTG OFC
(PDF) A MALHOTRA

1 DIR ARL
(PDF) RDRL SEE O
M FARRELL